Underground Mining Technology 2017 – M Hudyma & Y Potvin (eds)

doi:10.36487/ACG_rep/1710_29_Koupouli

Shear strength between cemented paste backfill and natural rock surface replicas

NJF Koupouli *University of Quebec, Canada*

T Belem *University of Quebec, Canada*

P Rivard *University of Sherbrooke, Canada*

Abstract

After placement underground, the physical–chemical and mechanical properties of cemented paste backfill (CPB) will evolve over time due to self-weight consolidation and binder hydration. This paper deals with an experimental investigation into the shear strength behaviour of the CPB–rock interfaces using a direct shear machine. Numerous shear tests were conducted. The rock interfaces were made from two natural rock surfaces (schist and granite) in SikaGrout® mortar replicas. Both frictional shear and shear bond strengths were determined. The results show that the shear strength at the schist interface (rougher) is higher than the one at the granite interface. The shear bond strength or cohesion and the interfacial angle of friction depend on the CPB curing time and the applied normal stress.

Keywords: *cemented paste backfill, natural rock surface, shear strength, cohesion, angle of friction*

1 Introduction

Cemented paste backfill (CPB) technology is increasingly and widely used in many underground mines throughout the planet and has become popular over the last two decades (e.g. Potvin et al. 2005; Belem & Benzaazoua 2008). CPB is obtained from mixing tailings with water and a binder. This technology was implemented in Canadian mines in the early 1990s (e.g. Landriault & Tenbergen 1995; Landriault et al. 1997; Nantel 1998). This popularity is partly due to the environmental directives implemented in many mining countries. The technology implies the reuse of at least 50% of the full stream tailings as CPB for underground mine stopes filling. The role of the CPB is to serve as secondary ground support (e.g. Mitchell 1989a; Belem et al. 2000a). Consequently, CPB can provide a stable working platform for miners, and it reduces the amount of open space that could potentially be filled with a collapse of the surrounding pillars (Barret et al. 1978). In order to retain the CPB during open stope filling, the structural barricades are designed to prevent any failure induced by high pressures generated by the saturated fill mass. In most cases, the stopes are filled in two sequences: a plug fill of a few metres high followed by the mass fill. The binder content in the plug fill is usually higher than the binder content in the mass fill. The plug fill is usually left between one and three days at rest prior to the mass filling in order to allow the water pore pressure dissipation and reduced pressure on the barricade. However, the proper design of a barricade requires a correct estimate of barricade loads which in turn depend on the stress distribution within the backfilled stope (Belem et al. 2013).

In many cases, the adjacent rock sidewalls actually help support the fill through interface shear strength and the arching phenomenon. Therefore, CPB and rock sidewalls may be mutually supporting (Mitchell 1989b). When arching occurs in a filled stope, the vertical stress at the bottom of the fill mass is lower than the overburden pressure due to horizontal stress transfer (Martson 1930; Terzaghi 1943). This pressure transfer is primarily associated with the frictional and/or cohesive interaction between CPB and the rock sidewall (Belem & Benzaazoua 2008). In situ measurements conducted by Le Roux et al. (2005) show that the porewater pressure on barricades is negligible after a few days. If the CPB permeability is very low and water does not drain out under gravity, no settlement of the CPB occurs (Belem et al. 2013). However, without any settlement, no shear stress can be mobilised at the CPB–rock sidewall interface and no arching

could occur. However, if the CPB desaturates just enough to enable negative pore pressures generation (Le Roux et al. 2005) this will in turn mobilise shear stresses at the fill–rock sidewall interface. The shear strength that can be mobilised at the interface will depend on the level of friction. This friction, in turn, is a function of the horizontal effective stress acting on the interface (Fourie et al. 2007). The determination of shear stress development will allow understanding of how the arching effect can occur (and thus stress relief on barricades). This effect can be taken into account during the preliminary backfill design process (De Souza et al. 2009). It is therefore necessary to investigate the shear strength parameters experimentally (interface cohesion or adhesion, interface friction angle, frictional shear strength, shear bond strength) and the shear stiffness of CPB–rock sidewall interfaces.

Very few experimental studies have been conducted on CPB–natural rock sidewall interface behaviour. One study on the shear behaviour of simulated backfill (SBkf)–limestone smooth interface was carried out by Nasir and Fall (2008), followed by another study on SBkf–concrete and brick interfaces (Fall & Nasir 2010). The normal stress was varied from 100 to 200 kPa and four different curing times were investigated (one, three, seven and 28 days) using a single Portland cement content of 4.5% (by dry mass of ground silica, namely SIL-CO-SIL 106, which is different from true tailings). The main conclusions were that, for the same stress conditions, the shear strength of the SBkf materials was greater than that of the SBkf–limestone/concrete/brick interfaces. The results obtained by these authors also suggested that the interfacial angle of friction (δ) of SBkf–limestone/concrete/brick interfaces was greater than 2/3 of the angle of internal friction (ϕ) of SBkf material ($\delta > 2/3\phi$). Indeed, Martson (1930) proposed that δ is ranged between $1/3\phi$ and $2/3\phi$, while Terzaghi (1943) considered that $\delta = \phi$. For the design of a backfilled stope with an exposed free face, Mitchell et al. (1982) made the assumptions that (i) the backfill–rock sidewall interfacial cohesion (C_b) is equal to the cohesive strength of the backfill material (*c*), and (ii) $\delta = \phi = 0$. Manaras (2009) performed direct shear tests on CPB–concrete interfaces. The CPB samples were prepared using the Brunswick Mine tailings. Barton's joint roughness coefficient (JRC) profiles were used for quantifying the joint walls' roughness (Barton 1973). The JRC values varied from three to 19. The normal stress ranged from 35 to 1,500 kPa and three different curing times were tested (14, 28 and 56 days). The CPB samples were prepared at 80% of solid content with three different binder contents (2.5, 5 and 8% by dry mass of tailings). The interfacial friction angle varied between 35 and 40°, when the CPB incorporates 2.5% binder content and the mixtures were cured from 14 to 28 days. This friction angle varied between 39 and 41° when the binder content was 5%. The friction angle varied between 41 to 50° when the binder content was increased to 7.5%. It was concluded that the interfacial friction angle δ and cohesion C_b increased with the amount of the binder, the wall roughness, and the curing time.

Although the results of these previous studies contribute to the understanding of interface phenomena, it remains that more investigation is needed for understanding the behaviour of interfaces between real cemented paste backfills and real rock surfaces. To the authors' knowledge, such a study has not been conducted to date. Hence, the main objective of this paper is to conduct a laboratory investigation into the shear stress–tangential displacement behaviour and the determination of shear strength parameters of early age CPB–granite and schist rock sidewall interfaces using a direct shear machine. Two curing times were tested: 14 and 28 days. The results of these tests will allow estimating the short-term shear strength that develops at the backfill–rock sidewall interface, and which is believed to be responsible for the arching effects occurrence in backfilled stopes. The obtained results will also be useful for better theoretical estimates of the pressure distribution in a backfilled stope using analytical solutions which take the arching effect into account (e.g. Aubertin et al. 2003; Li et al. 2005). The results may help understand the shear behaviour of early age backfill and analysing the shear strength at the interfaces of real backfill–rock surface.

2 Materials

2.1 Mine tailings sample

The tailings sample used in this study was taken from Casa Berardi mine (Hecla Mining Company, Quebec, Canada). This mine is located in northwest Quebec, Canada. The tailings were collected in barrels from the ore processing plant. After transferring to the lab, tailings barrels were first homogenised, then different small tailings samples were taken for the mineralogical analysis using X-ray diffractometer (XRD), grain size distribution, and chemical analysis using inductively coupled plasma-atomic emission spectrometer (ICP-AES).

The physical and mineralogical properties are presented in Table 1. The grain size distribution of the tailings was determined using a Malvern® Mastersizer S2000 laser particle size analyser. The Mastersizer uses laser diffraction for measuring the particle of the size from 0.06 to 879 µm (Figure 1).

Table 1 Physical and mineralogical properties of Casa Berardi's mine tailings

Parameter	Value	Mineral	Grade (%)
D_{10}	3.6 µm	Quartz	34.8
D_{30}	9 µm	Chlorite	12.3
D_{50} (d_{av})	19.3 µm	Ankerite	18.3
D_{60}	26.2 µm	Pyrite	2.7
D_{90}	120.7 µm	Albite	9.2
$P_{20\mu m}$	51%	Muscovite	22.7

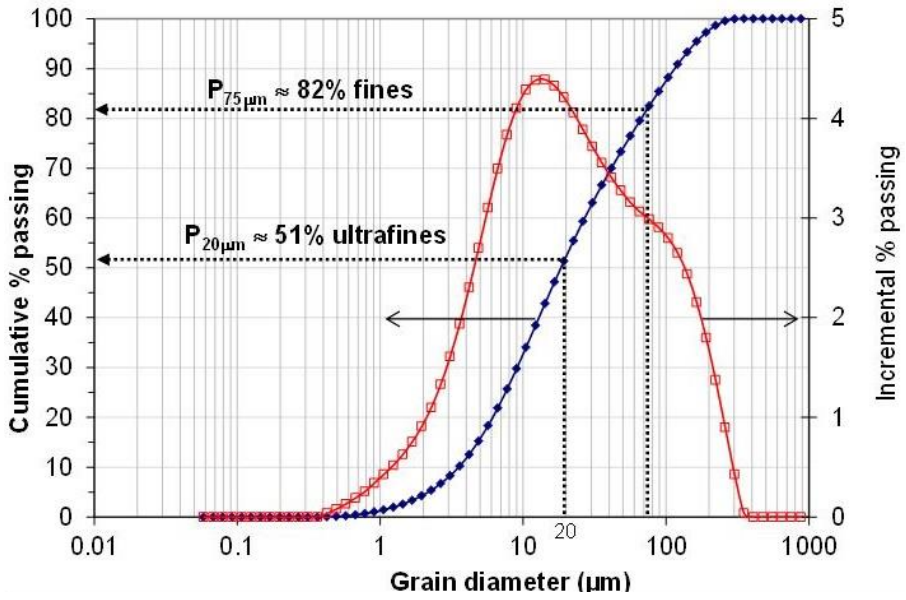

Figure 1 Grain size distribution curves of Casa Berardi mine tailings sample

2.2 Binder type

The binder used for backfill mixture preparation was provided by Lafarge North America and is a blend of 20% general use Portland cement (type GU) and 80% ground granulated blast furnace slag (GBFS). The binder content $B_{w\%}$ (= 100*M_{binder}/$M_{dry\text{-}tailings}$) was 5% by dry mass of tailings.

2.3 Natural surfaces moulding and rock wall mortar replicas preparation

Room-temperature-vulcanisation (RTV) silicone was used for reproducing the natural rock surfaces accurately. RTV silicone is first poured over the targeted surface portions using a squared frame and left to harden (Figures 2(a) and (b)). The RTV silicone used (commercial name of BLUESIL RTV 1556) is a two-component silicone elastomer (base and catalyst components) which cross-links at room temperature by poly-addition reaction. After curing time, it becomes a strong elastic material. Its low viscosity and shrinkage allows for the taking of any form. It is designed specifically for mould making.

Artificial rock surface mortar replicas were prepared by pouring a blend of SikaGrout® 212 and water (water-to-Sika ratio of 0.18, room temperature of approximately 23° ±2° C, and relative humidity ≥ 50%) over the previously obtained silicone mould and left to cure for 28 days (Figure 2(c)). SikaGrout® 212 is a high quality cement without shrinkage. It can be placed at a hardening or fluid state by simply adjusting the amount of water. After hardening, the natural rock mortar replicas are removed from the moulds, and will then be used as rock sidewall (Figures 2(d) and (e)). After 28 days of curing, the average unconfined compressive strength (UCS) was around 56 MPa. A total of four granite surfaces (G1 to G4) and four schist surfaces (S1 to S4) were moulded for the manufacture of SikaGrout® 212 artificial rock mortar replicas.

The surface of the specimens was characterised using surface roughness coefficient R_s (El Soudani 1978), which is defined as the ratio of the actual surface area to the projected surface area ($R_s = A_t/A_n$). The surface roughness coefficient R_s varies from 1.051 to 1.070 for granite surfaces, and from 1.088 to 1.185 for schist surfaces. Belem et al. (2000b) proposed the specific surface roughness coefficient SR_s (= 100*[R_s – 1]) to better capture and quantify the amount of surface roughness compared to its nominal projected area (A_n). The specific surface roughness coefficient SR_s varies from 5.1 to 7.0% for granite surfaces, and from 11.1 to 18.5% for schist surfaces. It may therefore be stated that the schist surfaces are rougher, in the strict sense, than the granite surfaces. It should be mentioned that the maximum and minimum heights on the schist surface (amplitude of the surface topography) are greater than the granite surface and that the schistosity is more or less directional. This is not the case with the granite surface, which exhibits rather isotropic morphology.

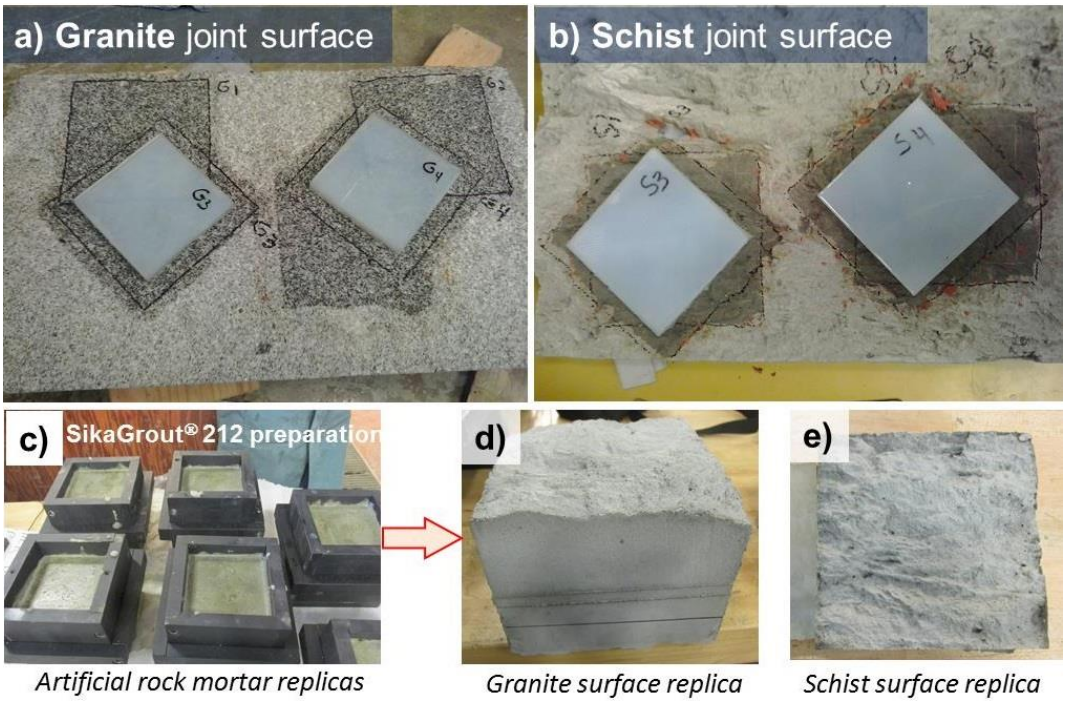

Figure 2 Natural rock surface moulding and mortar replicas preparation: (a) Granite surface with hardened RTV silicone moulding; (b) Schist surface with RTV silicone moulding; (c) Mortar replicas (artificial rock) preparation using SikaGrout® 212; (d) Artificial granite mortar replica; and, (e) Artificial schist mortar replica

2.4 Direct shear apparatus

The direct shear tests were performed on cemented paste backfill–artificial rock wall interfaces in order to assess the frictional shear strength parameters and shear bond strengths. The direct shear apparatus (Figure 3) generates pressure using a hydraulic pump, and can operate at low pressure (with a maximum of 7 MPa) or high pressure (with a maximum of 21 MPa). This pressure allows the sample shearing through the relative displacement of two half-shear boxes (one fixed and one movable). The fixed lower half-box contains the artificial rock specimen, and the upper movable half-box contains the CPB specimen. The shear box is connected to a digital control system composed of a computer and software, and a data acquisition system.

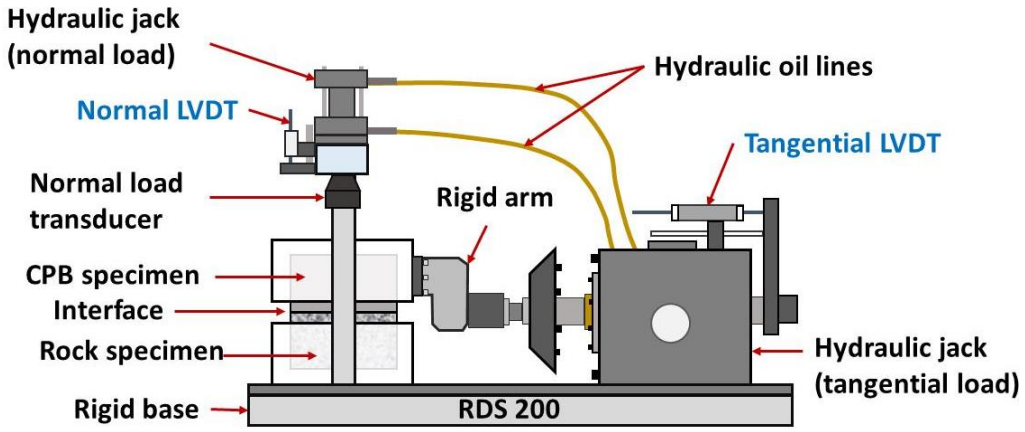

Figure 3 Direct shear test machine RDS-200 from GCTS (from Koupouli et al. 2015)

3 Experimental program

3.1 Paste backfill–rock mortar replica specimens preparation

For the cemented paste backfill preparation, the required masses of tailings, water and binder (20% of type GU Portland cement and 80% of GBFS) were mixed and kneaded using a Hobart mixer for about 10 minutes. The slump height was about ≈ 180 ± 2 mm (≈ 7 ± 0.08 in.), which corresponds to a solid mass concentration $C_{w\%}$ of 76% (= 100*(100/[100+w%]); where w% is the water content). The fresh CPB is then poured over the surface of artificial rock mortar replica using 120 × 120 mm section and 65 mm height PVC moulds (Figures 4(a) & (b)), in order to create the interface between CPB and rock wall (Figure 4(c)). Once cast, the CPB samples were cured in a humid chamber at room temperature (23 ± 2° C) and > 90% relative humidity (RH). The rock mortar replicas were pre-cut to the same size as the CPB specimens. The final dimensions of each assembled specimen (CPB–rock wall mortar replica) after demoulding were a 116 × 116 mm section, 120 mm high. The average unconfined compressive strength (UCS) values of the CPB triplicate specimens were 522 kPa at 14 days of curing and 1,212 kPa at 28 days of curing.

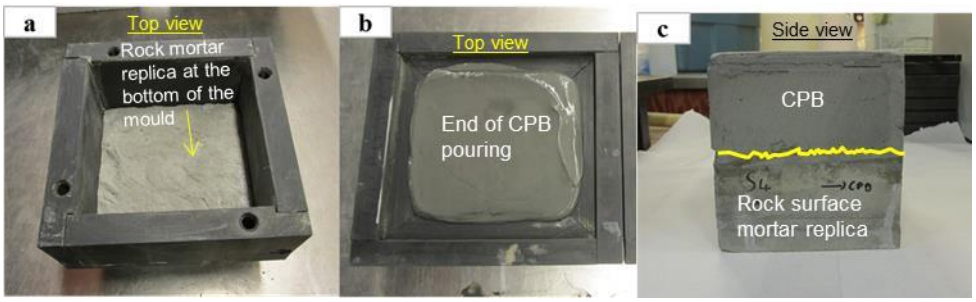

Figure 4 CPB and rock surface mortar replicas preparation: (a) Rock mortar replica at the bottom of the mould; (b) Pouring of CPB on top of the rock mortar replica; and (c) Demoulded specimen

3.2 Shear test on backfill–artificial rock mortar replica interfaces

3.2.1 Friction testing program

This testing was performed on the granite rock interfaces (G1 and G3) and the schist rock interfaces (S1 and S4). For each curing time and for each interface, three CPB–rock surface specimens were used for three different applied normal stresses (50, 100 and 150 kPa). A constant shear rate of 1 mm/min and a total shear displacement of 10 mm were used. The shear stress–shear displacement curves were used for determining the failure envelope and its corresponding criterion.

3.2.2 Interfacial shear bond testing program

Only one specimen cured at 14 days was used at a low applied normal stress of 5 kPa for the determination of the interfacial shear bond strength. The CPB–mortar rock interfaces were G1, G2 and G3 for the granite surface, and S1, S2 and S3 for the schist surface. A very low constant shear rate of 0.05 mm/min and a total shear displacement of 8 mm were used.

4 Results and discussion

4.1 Friction test results

The shear test results can be represented by graphs of shear stress τ–shear displacement u curves, normal displacement v–shear displacement u curves and peak shear stress τ_p–normal stress σ_n curves. The τ_p–σ_n curves are used for determining the failure envelope according to the Mohr–Coulomb criterion:

$$\tau_p = c_x + \sigma_n tan\varphi_j \quad (1)$$

where:

c = cohesion.

x = a (c_a) for apparent or adhesion.

x = b (c_b) for bond.

φ_j = interface angle of friction.

It should be mentioned that the value of the peak shear stress τ_p at a normal stress σ_n = 0 corresponds to (i) the apparent cohesion or adhesion (c_x = c_a) of a non-bonded joint or interface, and (ii) the bonding cohesion (c_x = c_b) of a bonded joint.

4.1.1 Shear stress–shear displacement curves

For each type of rock mortar replica, only the results from one surface were presented, namely G1 for the granite surface and S1 for the schist surface (Figures 5 and 6). As can be seen, the shear stress–shear displacement curves can be divided into four stages (see, for example, Figure 5(a)):

- Stage one corresponds to an initial peak shear stress associated with the shear bond strength. Indeed, at this stage, the shear stress increases with the shear displacement until it reaches an initial peak at a shear displacement ranging from 2 to 3 mm. According to Kodikara and Johnston (1994), this stage could correspond to the breakage of the cement bonding.
- At stage two, a slight decrease is observed in the shear stress as the shear displacement increases. This happens after the breakage of the surface bonding and that produces a slip on the interface of the two surfaces.
- Stage three is characterised by an increase in the shear stress as the shear displacement increases until it reaches the interface peak shear stress (friction). This happens because, while the shear

displacement increases, the interface asperities contact area or the contact at the CPB–rock interface decreases. This reduction causes the increase of the contact load and stress. This increase in load and stress is primarily due to the contact between the CPB and rock surface asperities until the local stress on the CPB major asperity (critical stress) exceeds its shear strength. As the CPB major asperity cannot carry the load at this critical stress, it fails. However, some strong CPB asperities may not have been damaged during this stage.

- At stage four the surface of the CPB has suffered the most damage because of its low strength compared to the mortar rock (schist or granite). After the CPB asperities crushing, slippage occurs at the CPB–rock interface producing a decrease in shear stress observed in the shear stress–shear displacement curves.

After stage four, some stick-slip behaviour can be observed, but is mostly characterised by a relatively constant shear stress, or a slight decrease in shear stress, as the shear displacement increases. This can result from both sliding – overriding at the interface and damage of some weaker asperities during shearing (Indraratna & Jayanathan 2005). This can be due to: (i) the contribution of some undamaged strong asperities to shear stress, and (ii) the CPB particles (tailings) slide or roll over the mortar rock, and the presence of friction between tailings particles themselves and the mortar rock surface. Indeed, the observation of the mortar rock interface after testing confirms this assumption, because much of the CPB's asperities have broken.

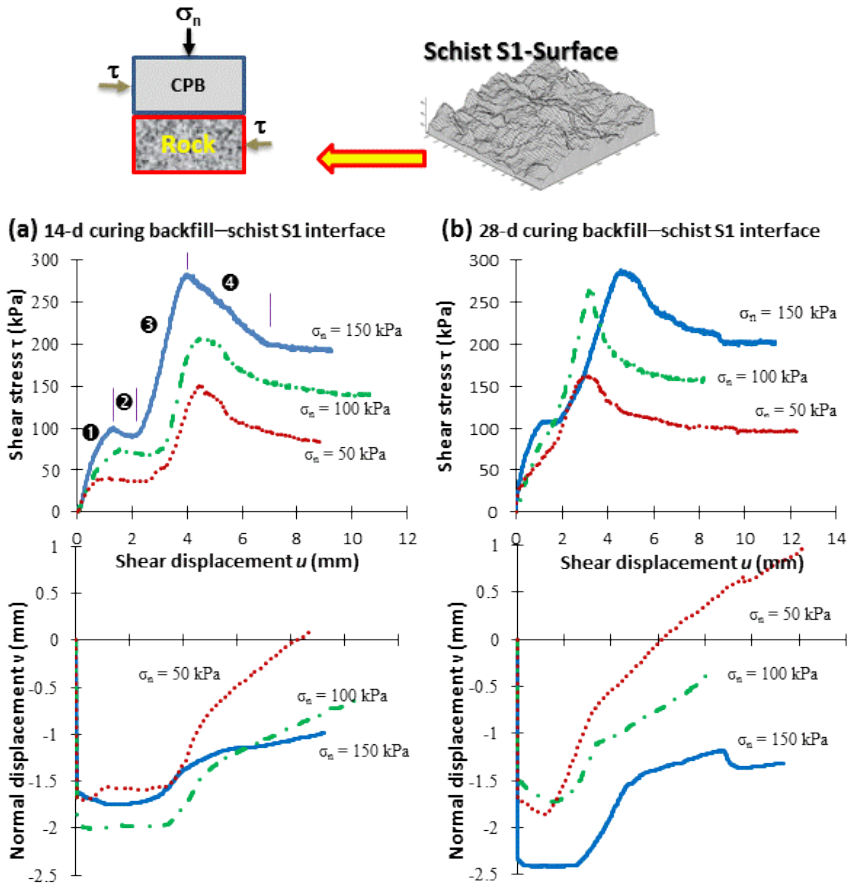

Figure 5 **Shear stress–shear displacement–normal displacement curves: (a) Backfill cured at 14 days and bonded with schist S1 surface; and, (b) Backfill cured at 28 days and bonded with schist S1 surface**

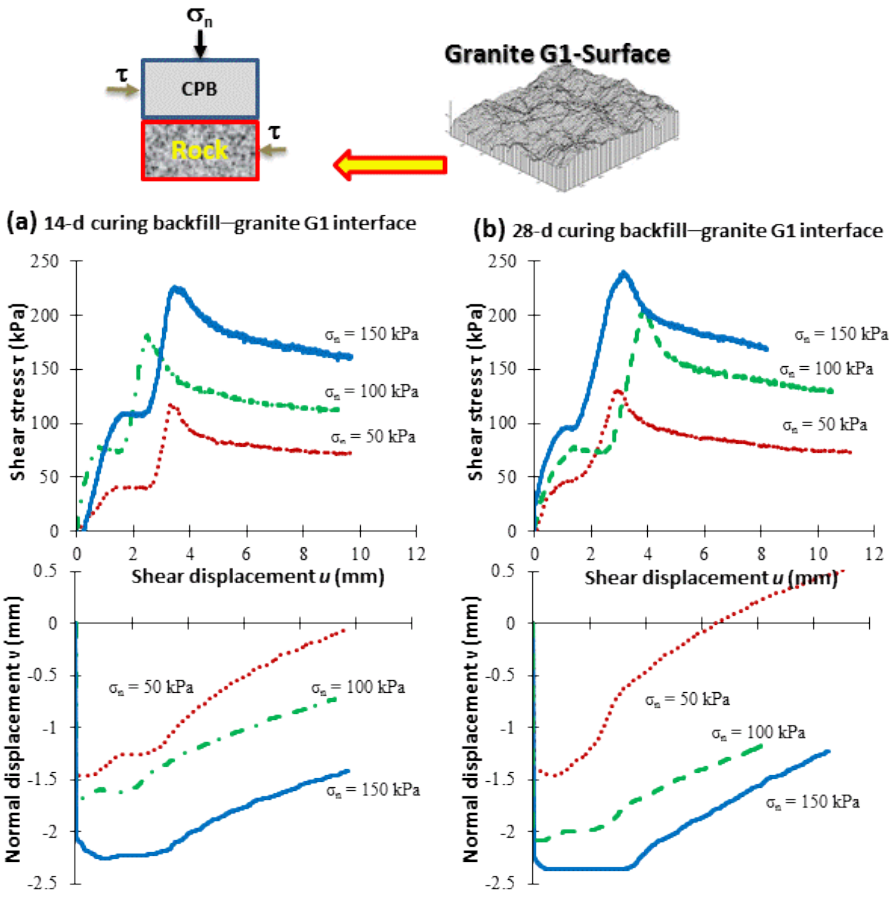

Figure 6 Shear stress–shear displacement–normal displacement curves: (a) Backfill cured at 14 days and bonded with schist S1 surface; and, (b) Backfill cured at 28 days and bonded with schist G1 surface

For the normal displacement–shear displacement curves, three stages can be observed (see, for example, Figure 5a)). The first part is a significant contraction corresponding to the normal stress application. This initial normal displacement corresponds to the maximum compressibility that the CPB can withstand under the applied normal stress. It was observed that this initial normal displacement increases as the applied normal stress increases (σ_n = 150 kPa). The second part of the normal displacement–shear displacement curves shows a relatively constant normal displacement in the range 0–3 mm. Note that this part corresponds to stages one and two of the shear stress–shear displacement curves, which is characterised by a cement bond between CPB and mortar rock. Therefore, no normal displacement was observed during this stage because the asperities interaction has not started. The last part is characterised by dilation. This is mainly due to the asperities interaction between CPB and mortar rock. The rolling and sliding of CPB particles over the mortar rock surface increase normal displacement, as discussed earlier.

4.1.2 Shear strength parameters

Table 2 summarises the cohesive strength and the interfacial angle of friction for granite G1 and G3 and for schist S1 and S4. The main observation is that the variation in the shear strength depends mostly on the mortar rock surface roughness. In addition, the bonding cohesion c_b varies in the range 65–115 kPa, while the interfacial angle of friction φ_j varies in the range 45–52°. These results show that for a given interface, the CPB curing time does not have a great impact on the values of the interfacial shear parameters, contrary to surface roughness. A recent study by Koupouli (2015) showed that for the CPB matrix, having the same characteristics as those presented in this paper, the internal cohesion *c'* varies from 130–340 kPa,

while the internal angle of friction ϕ' varies from 39–43°. Therefore, according to the results of this study, $c' > c_b$ and $\phi' < \varphi_j$.

Table 2 Shear strength parameters of granite (G1 and G3) and schist (S1 and S4) surface mortar replicas

	Interface bonding cohesion c_b (kPa)		Interface angle of friction φ_j (°)	
	14 day curing	28 day curing	14 day curing	28 day curing
Granite G1	68	78	46	49
Granite G3	65	68	51	45
Schist S1	90	115	51	52
Schist S4	82	70	46	51

4.2 Interfacial shear bond test results

Figure 7 presents the shear stress–shear displacement curves for the granite (Figure 7(a)) and schist (Figure 7(b)) interfaces. In general, two stages can be observed from this figure. A first elastic-plastic loading with a plateau (stage ①) followed by a stress increase until a peak was reached (stage ②) before the stress drop (stress softening stage). The peak shear stress corresponds to the interface shear bond strength (or adhesive strength). Two strength parameters can be obtained, namely the cement bond strength (τ_b,stage ①) and the peak shear stress (τ_p,stage ②) observed at the mortar rock and CPB interface during frictional sliding after cement bond breakage. Taking into account the uncertainties of the measures, the shear bond strength τ_b is approximately 10 kPa for the granite interface G1, 11 kPa for granite G2, and 17 kPa for the granite G3 mortar replicas. For the interface of schist S1, S2 and S3 mortar replicas, τ_b is approximately 10 kPa. This shear bond strength is reached when the shear displacement is between 1 and 2 mm.

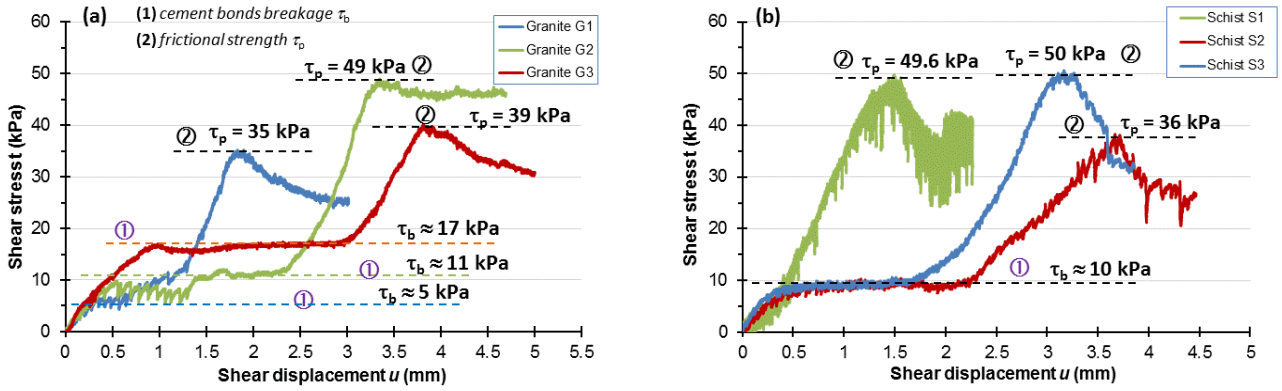

Figure 7 Interfacial shear bond curves at the CPB–mortar rock interface: (a) Granite G1, G2 and G3; and, (b) Schist S1, S2 and S3 (14 day curing time)

5 Concluding remarks

This paper investigated the impact of paste fill (CPB) curing time and roughness of mortar replicas of natural rock surfaces of schist and granite on the shear strength parameters (i.e. cement bonding cohesion c_b, cement bond strength τ_b, interfacial angle of friction φ_j, and peak shear strength τ_p) of CPB–mortar replica interfaces. In general, it appears that the CPB curing time would have no impact on these parameters, but rather the roughness at the interface. From the results obtained, the following conclusions can be drawn:

- The shear strength τ_p of the granite surface mortar replicas (G1 and G3) varies from 120–245 kPa.

- For the schist interfaces (S1 and S4), which are rougher than the granite interfaces, the shear strength τ_p varies from 130–293 kPa.
- The cement bond cohesion c_b varies in the range 65−115 kPa (lower than the internal cohesion c' of the CPB matrix).
- The interfacial angle of friction φ_j varies in the range 45−52° (higher than the internal angle of friction ϕ' of the CPB matrix).
- The shear bond strength τ_b varies between 10 and 17 kPa for granite and schist surface mortar replicas.

Acknowledgement

This research was financially supported through the Natural Sciences and Engineering Research Council of Canada (NSERC) Discovery Grant and the Research Institute on Mining and the Environment. The authors are grateful for their support. The authors also acknowledge Danick Charbonneau, technician at the rock mechanics lab of the University of Sherbrooke for his valuable help and support. The authors also acknowledge Lafarge North America Inc. for kindly providing us with all the Portland cement and supplementary cementitious materials.

References

Aubertin, M, Li, L, Arnold, S, Belem, T, Bussiere, B, Benzaazoua, M & Simon, R 2003, 'Interaction between backfill and rock mass in narrow stopes', in PJ Culligan, HH Einstein & AJ Whittle (eds), *Proceedings of SoilRock2003: 12th Panamerican Conference on Soil Mechanics and Geotechnical Engineering and 39th U.S. Rock Mechanics Symposium*, vol. 1, Verlag Glückauf GmbH, Essen, pp. 1157–1164.

Barret, JR, Coulthard, MA & Dight, PM 1978, 'Determination of fill stability, mining with backfill'*, Proceedings of the 12th Canadian Rock Mechanics Symposium*, Canadian Institute of Mining and Metallurgy, Montreal, pp. 85–91.

Barton, NR 1973, 'Review of a new shear strength criterion for rock joint deformation', *Engineering Geology*, vol. 7, pp. 287–332.

Belem, T & Benzaazoua, M 2008, 'Design and application of underground mine paste backfill technology', *Geotechnical and Geological Engineering*, vol. 26, no. 2, pp. 148–174.

Belem, T, Benzaazoua, M & Bussière, B 2000a, 'Mechanical behaviour of cemented paste backfill', *Proceedings of the 53rd Canadian Geotechnical Conference: Geotechnical Engineering at the Dawn of the Third Millennium*, vol. 1, Canadian Geotechnical Society, Montreal, pp. 373–380.

Belem, T, Homand-Etienne, F & Souley, M 2000b, 'Quantitative parameters for rock joint surface roughness', *Rock Mechanics and Rock Engineering*, vol. 33, no. 4, pp. 217–242.

Belem, T, Benzaazoua, M, El-Aatar, O & Yilmaz, E 2013, 'Effect of drainage and the pore water pressure dissipation on the backfilling sequencing', *Proceedings of the 23rd World Mining Congress*, Canadian Institute of Mining, Metallurgy and Petroleum, Westmount, 10 p.

de Souza, E, Archibald, J & Beauchamp, L 2009, 'Compilation of industry practices for control of hazards associated with backfill in underground mines - Part I surface and plant operations', in M Diederichs & G Grasselli (eds), *Proceedings of the 3rd Canada-US Rock Mechanics Symposium: RockEng09,* Canadian Rock Mechanics Association, 12 p.

El Soudani, SM 1978, 'Profilometric analysis of fractures', *Metallography*, vol. 11, pp. 247–336.

Fall, M & Nasir, O 2010, 'Mechanical behaviour of the interface between cemented tailings backfill and retaining structures under shear loads', *Geotechnical and Geological Engineering*, vol. 26, no. 6, pp. 779–790.

Fourie, AB, Fahey, M & Helinski, M 2007, 'Using effective stress theory to characterize the behaviour of backfill', *CIM Bulletin*, vol. 100, no. 1103, pp. 1–9.

Indraratna, B & Jayanathan, M 2005, 'Measurement of pore water pressure of clay-filled rock joints during triaxial shearing', *Geotechnique*, vol. 55, no. 10, pp. 759–764.

Kodikara, JK & Johnston, IW 1994, 'Shear behaviour of irregular triangular rock-concrete joints', *International Journal of Rock Mechanics and Mining Sciences Abstracts*, vol. 31, no. 4, pp. 313–322.

Koupouli, NJF 2015, *Comportement mécanique des remblais en pâte cimentés en compression et en cisaillement et étude du frottement aux interfaces remblai-remblai et remblai-roche*, Master's thesis in mineral engineering, University of Quebec, Quebec, 222 p.

Koupouli, NJF, Belem, T, Rivard, P & Effenguet H 2015, 'Direct shear tests on cemented paste backfill–rock wall and cemented paste backfill–backfill interfaces', *Journal of Rock Mechanics and Geotechnical Engineering*, vol. 8, no. 4, pp. 472–479.

Landriault, DA & Tenbergen, R 1995, 'The present state of paste fills in Canadian underground mining', in FP Hassani & P Mottahed (eds), *Proceedings of the 97th Annual General Meeting of the CIM Rock Mechanics and Strata Control Session*, Canadian Institute of Mining, Metallurgy and Petroleum, Westmount, pp. 229–238.

Landriault, DA, Verburg, R, Cincilla, W & Welch, D 1997, 'Paste technology for underground backfill and surface tailings disposal applications', short course notes, technical workshop held on 27 April 1997, Canadian Institute of Mining and Metallurgy, Montreal, 120 p.

Le Roux, K-A, Bawden, WF & Grabinsky, MWF, 2005, 'Field properties of cemented paste backfill at the Golden Giant mine', *Transactions of the Institution of Mining and Metallurgy, Section A: Mining Technology*, vol. 114, no. 2, pp. 65–86.

Li, L, Aubertin, M & Belem, T 2005, 'Formulation of a three dimensional analytical solution to evaluate stress in backfilled vertical narrow openings', *Canadian Geotechnical Journal*, vol. 42, no. 6, pp. 1705–1717.

Manaras, S 2009, *Investigations of Backfill – Rock Mass Interface Failure Mechanisms*, master's thesis, Queen's University, Kingston.

Martson, A 1930, 'The theory of external loads on closed conduits in the light of latest experiments', *Bulletin 96, Iowa Engineering Experiment Station*, vol. 28, no. 38.

Mitchell, RJ 1989a, 'Stability of cemented tailings backfill', *Computer and Physical Modelling in Geotechnical Engineering,* A.A. Balkema, Rotterdam, pp. 501–507.

Mitchell, RJ 1989b, 'Model studies on the stability of confined fills', *Canadian Geotechnical Journal*, vol. 26, no. 2, pp. 210–216.

Mitchell, RJ, Olsen, RS & Smith, JD 1982, 'Model studies on cemented tailings used in mine backfill', *Canadian Geotechnical Journal*, vol. 19, no. 1, pp. 14–28.

Nantel, J 1998, 'Recent developments and trends in backfill practices in Canada', in M Bloss (ed.), *Proceedings of the 6th International Symposium on Mining with Backfill: Minefill 1998*, The Australasian Institute of Mining and Metallurgy, Melbourne, p. 11–14.

Nasir, O & Fall, M 2008, 'Shear behaviour of cemented pastefill-rock interfaces', *Engineering* Geology, vol. 101, no. 3–4, pp. 146–53.

Potvin, Y, Thomas, E & Fourie, A (eds) 2005, *Handbook on Mine Fill*, Australian Centre for Geomechanics, Perth.

Terzaghi, K 1943, *Theoretical Soil Mechanics*, John Wiley & Sons, Inc., New York.